ELSEVIER

Catalysis Today 75 (2002) 305–315

CATALYSIS TODAY

www.elsevier.com/locate/cattod

Honeycomb-supported perovskite catalysts for high-temperature processes

Lyubov A. Isupova*, Galina M. Alikina, Sergei V. Tsybulya, Aleksei N. Salanov, Nataliya N. Boldyreva, Elena S. Rusina, Izabella A. Ovsyannikova, Vladimir A. Rogov, Rimma V. Bunina, Vladislav A. Sadykov

Boreskov Institute of Catalysis, SB RAS, Pr. Lavrentieva, 5, 630090 Novosibirsk, Russia

Abstract

Pechini route [US Patent No. 3,330,697 (1967)] was used for supporting perovskite-like systems on thin-wall corundum honeycomb support to prepare catalysts for high-temperature processes of methane combustion and selective oxidation into syngas. In this preparation, the surface of corundum monoliths walls was shown to be covered by strongly adhering porous perovskite layer formed by rounded crystals. At high temperatures when pore diffusion is expected to affect catalysts performance in fast reactions, this spatial distribution of the active component could be attractive. In the kinetically controlled region of methane oxidation, samples prepared via Pechini route possess activity comparable with that of samples made via support wet impregnation with mixed nitrate solutions, when an active component is uniformly distributed across the wall thickness. Corundum-supported lanthanum manganite and ferrite are the most active in the reaction of methane combustion, while its selective oxidation into syngas effectively proceeds on supported lanthanum cobaltite and nickelates. Corundum-supported perovskites are more thermally stable as compared with those on γ-alumina support.

Keywords: Methane oxidation; Perovskites; Honeycomb corundum-supported catalysts

1. Introduction

High-temperature catalytic processes such as deep oxidation of methane (DOM) and partial oxidation of methane (POM), its autothermal reforming, fuels combustion, selective oxidation of paraffins into olefins, etc. are now among the most rapidly developing fields in the heterogeneous industrial catalysis. Complex oxides with perovskite structure were shown to be promising for such applications [1–4]. For those processes occurring at short contact times, the monolith honeycomb shape of catalysts is often required. The traditional approach in technology of monolithic catalysts preparation consists in supporting active components on the refractory monolithic carrier [5]. To avoid interaction between the active component and support at the preparation stage, to ensure the uniformity of its distribution in the monolith channels as well as to achieve a reasonably high level of loading, method developed by Pechini [6] seems to be promising. Since up to date it has not been applied to the catalyst technology, the present paper aims at covering this gap for the case of supported monolithic perovskites.

* Corresponding author. Tel.: +7-3832-343-764; fax: +7-3832-343-056.
E-mail address: isupova@catalysis.nsk.su (L.A. Isupova).

0920-5861/02/$ – see front matter
PII: S0920-5861(02)00083-4

2. Experimental

2.1. Catalyst preparation

Supported $LaMeO_3$ (Me = Mn, Co, Fe, Ni, Cu) perovskites were prepared by impregnation of thin (thickness ~0.25 mm) wall monolithic corundum-support with triangular channels about 1.5 mm in size, specific surface area ~4 m^2/g, integral pore volume 0.35 cm^3/g and mean pore radius ~0.12 μm [4] by solutions of nitrates salts (room temperature saturated nitrate solutions were mixed in required proportions) with added citric acid and ethylene glycol [6]. After impregnation and drying at room temperature in the air flow, a film of polymerized metal–ether complexes strongly adhering to the monolithic support walls is formed. After annealing at 200–250 °C, the organic residue is burned and perovskite precursor is formed. According to the thermal analysis data, the processes of the gases evolution from that precursor at air

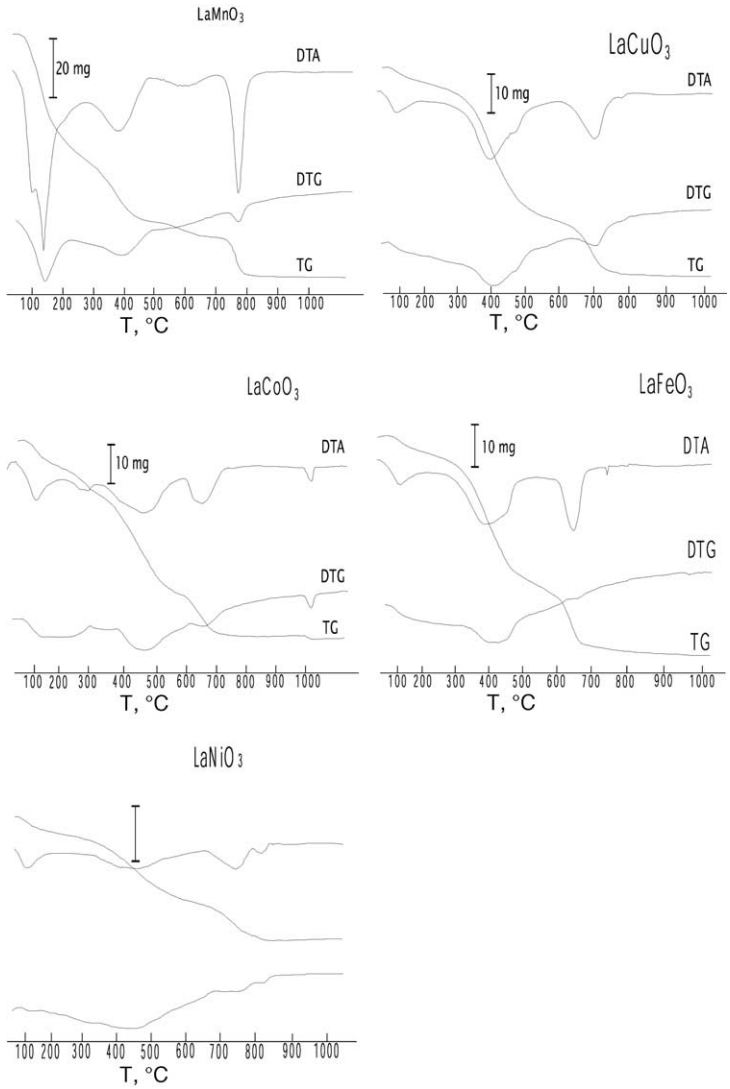

Fig. 1. TA of perovskite precursors.

annealing are completed only at temperatures exceeding 700 °C (Fig. 1). Hence, this temperature was chosen as a minimum catalysts calcination temperature. To study the catalyst thermal stability, samples were calcined for 4 h at 900 and 1100 °C. To improve the catalysts activity, they were promoted by Pt and Pd (∼0.2 wt.%) supported from nitrate solutions. For comparison, supported perovskites were also obtained by impregnation of the same support by mixed nitrate solutions either pure or with added citric acid (16 g/100 cm^3) followed by their drying and calcination. In one impregnation about 17 ± 2 wt.% of perovskite was supported.

2.2. Catalyst characterization

The methane oxidation activity of all the catalysts in methane combustion was estimated at the atmospheric pressure in the tubular integral plug-flow reactor with 16 mm i.d. fed by the gas mixture containing 0.5% CH_4 + 5% O_2 in He. The reactor was loaded with a piece of monolith (4–5 mm in length). The inlet and outlet gas concentrations were analyzed by GC. A relative contact time, τ, defined as a ratio of the catalyst layer volume (cm^3) to the flow rate (cm^3/s) was 0.25 s.

Methane conversion and CO selectivity in the POM reaction were determined at the atmospheric pressure in the tubular integral flow reactor with 7 mm i.d. loaded with a piece of monolith (∼10 mm length) at τ = 1 s with the 1% CH_4 + 0.5% O_2 in He inlet gas mixture composition.

The X-ray diffraction patterns were obtained with a URD-6 diffractometer using Cu Kα radiation. The 2θ scan region was 10–70°. Typical particle sizes were estimated from the broadening of 4 0 0 diffraction peak (cubic index) not splitted due to the hexagonal distortion of the perovskite structure.

The X-ray microanalysis (X-ray beam diameter ca. 1–2 mm) was carried out on a MAP-3 machine for corundum-supported $LaMnO_3$ catalysts prepared either by usual impregnation or via Pechini route and calcined for 4 h at 700–1100 °C. The characteristic Mn Kα, La Lα and Al Kα radiations were registered while moving beam across the wall thickness.

The textural features of supported perovskites were studied by TEM with a JEM-2010 machine (resolution limit is about 0.14 nm) and by SEM with a BS-350 machine (resolution limit is about 5–10 nm).

The thermal analysis was carried out on a DQ-1500 device. Samples (200 mg) were heated with a ramp of 10°/min up to 900 °C under atmosphere.

TPR studies with H_2 as reductant were performed for 0.25–1 mm samples fraction using a flow installation equipped with the thermal conductivity detector. Prior to reductions, samples were pretreated in O_2 for 0.5 h at 500 °C followed by cooling in O_2 to room temperature. The reduction gas was 10% H_2 in Ar flowing at 40 cm^3/min (STP). Samples (50–150 mg) were heated with the rate of 10°/min up to 900 °C.

The differential dissolution method of phase analysis was carried out using a BAIRD spectrometer and procedures earlier described in detail [7].

The samples pore structure was characterized by the high pressure mercury porometry (HPM) using an Auto-Pore 9200 machine, and the specific surface area (S_{sp}) was determined by a routine BET procedure using the Ar thermal desorption data.

3. Results and discussions

3.1. The phase composition and texture of supported perovskites

According to X-ray data, the perovskite precursors formed after burning the organic polymer are amorphous, which agrees with the data of Ref. [8]. Anions (probably, including even admixtures of starting salts) appear to be retained in the precursor, since its further heating is accompanied by the gases evolution (Fig. 1). Calcination of unsupported $LaMeO_3$ (Me = Fe, Mn) precursors at 800 °C leads to the formation of well-crystallized perovskites particles with the typical sizes ca. 80–100 nm. In the calcined precursors containing cobalt, nickel and copper cations, simple oxide admixtures (resp., Co_3O_4 [JCPDS 43-1003], NiO [JCPDS 44-1159], CuO [JCPDS 05-0661]) were revealed as well. The specific surface area for thus prepared bulk perovskites calcined at 800 °C was 13 m^2/g (for Me = Fe, Mn, Co, Ni) and 3 m^2/g (for Me = Cu), respectively.

In the case of corundum-supported samples, perovskite phases were observed after annealing at lower (starting from 700 °C) temperatures. At this temperature, the typical X-ray particle sizes are ∼10–30 nm, being constant up to 1100 °C for ferrites, manganites

Table 1
Phase composition, structure modification, X-ray particle size for perovskite oxides supported on corundum honeycomb carrier by Pechini route, depending on catalysts calcination temperature, T (°C)

Perovskite oxide	Phase composition, structure modification and X-ray particle size (nm) for catalysts calcined at		
	700 °C	900 °C	1100 °C
$LaCoO_3$	Perovskite, cubic, ∼13 nm, spinel	Perovskite, cubic, 16 nm, spinel	Perovskite, cubic, 80 nm, spinel
$LaCoO_3$[a]	–	–	Perovskite, cubic, 20 nm, spinel
$LaFeO_3$	Perovskite, orthorhombic, ∼12 nm	Perovskite, orthorhombic, ∼14 nm	Perovskite, orthorhombic, ∼18 nm
$LaMnO_3$	Perovskite, hexagonal, ∼20 nm	Perovskite, hexagonal, ∼25 nm	Perovskite, hexagonal, ∼30 nm
$LaNiO_3$	Perovskite, cubic, <10 nm	Perovskite, cubic, 12 nm, NiO, La_2O_3	Perovskite, cubic, 60 nm, spinel
$LaCuO_3$	Perovskite, cubic, 14 nm	Perovskite, cubic, 14 nm, CuO	Perovskite, cubic, 16 nm, spinel

[a] $LaCoO_3$ prepared by usual impregnation from nitrate or nitrate with citrate acid solutions.

and cuprates of lanthanum (Table 1). For supported lanthanum manganites and ferrites, the type of structure (hexagonal and orthorhombic, respectively) corresponds to stable modifications included in JCPDS files, though some cell contraction is observed (Table 2). In the case of cuprates, nickelates and cobaltites, instead of a stable hexagonal phase, a cubic modification was revealed, and additional spinel peaks were detected for catalysts calcined at 1100 °C (Tables 1 and 2). Hence, for the latter systems, pronounced interaction between the active component and support certainly take places. Moreover, according to differential dissolution data for samples calcined at 1100 °C (not shown here for brevity), all supported perovskite phases are modified by aluminum cations, their content increases from 5 to 19% in the order Fe < Mn < Co < Ni < Cu. It implies that at the impregnation stage followed by heating up to 200 °C, a part of support is dissolved in the acidic polymerized solution, which can be facilitated by a strong complexation ability of mixed citric acid–ethylene glycol ethers. After precursor decomposition and calcination, a part of aluminum cations enters into metastable perovskite-like solid solution, thus effecting their structural features, while another part (∼1–2 wt.%) is segregated at the surface of perovskite particles as amorphous oxide patches easily dissolved in the course of differential dissolution analysis even

Table 2
JCPDS and experimental data on perovskite's parameters

Oxide	JCPDS number	JCPDS parameters (Å)	Experimental parameter for supported catalysts calcined at 1100 °C (Å)
$LaCoO_3$	[25-1060] hexagonal (rhombohedral)	$a = 5.441$, $c = 13.088$	$a = 3.792(1)$
$LaCoO_3$[a] nitrate			$a = 3.797(1)$
$LaCoO_3$[b] citrate			$a = 3.800(2)$
$LaFeO_3$	[15-148] orthorhombic	$a = 5.556$, $b = 5.565$, $c = 7.862$	$a = 5.523(5)$[c], $b = 5.549(3)$, $c = 7.810(5)$
$LaMnO_{3.15}$	[32-484] hexagonal (rhombohedral)	$a = 5.523$, $c = 13.324$	$a = 5.485(3)$, $c = 13.333(7)$
$LaNiO_3$	[34-1181] hexagonal (rhombohedral)	$a = 5.451$, $c = 6.564$	$a = 3.797(1)$
$LaCuO_{3-\delta}$	[25-0291] hexagonal (rhombohedral)	$a = 5.502$, $c = 13.22$	$a = 3.794(1)$
$LaAlO_3$	[31-0022] hexagonal (rhombohedral)	$a = 5.364$, $c = 13.11$	–
$CoAl_2O_4$	[44-160] cubic	8.104	8.094(2)
$AlCo_2O_4$	[33-814]	8.086	
Co_3O_4	[42-1467]	8.0837	
$CuAl_2O_4$	[33-0448] cubic	$a = 8.075$	$a = 8.078(2)$
$NiAl_2O_4$	[10-0339] cubic	$a = 8.048$	$a = 8.032(3)$

[a] Catalyst prepared by impregnation from nitrate solution.
[b] Catalyst prepared by impregnation from citrate solution.
[c] $a = 3.895(5)$ Å in cubic cell.

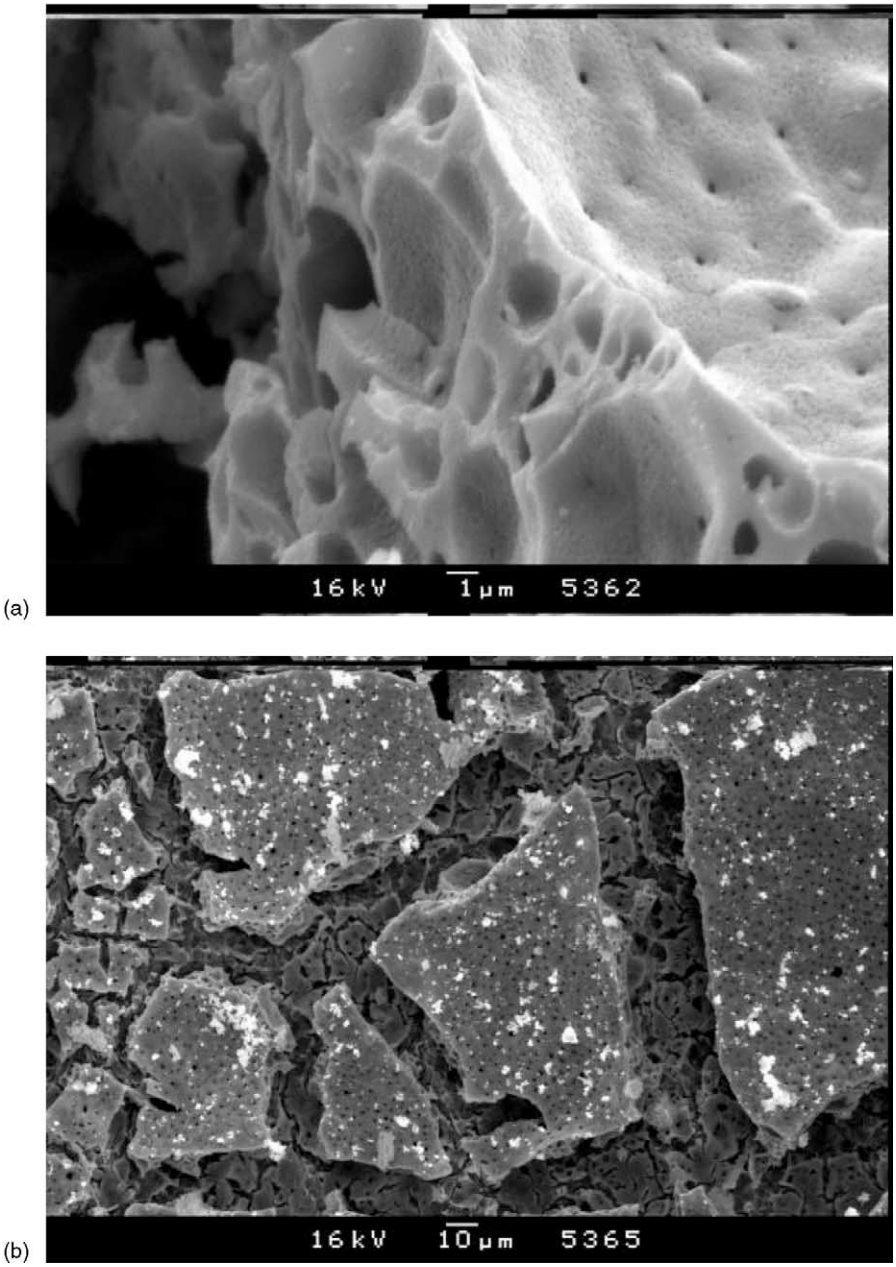

Fig. 2. SEM data on $LaMnO_3$ film: side view at cut (a) and view from above (b).

at room temperature. This admixture probably corresponds to bright patches with a low electron density revealed at the surface of perovskite particles by SEM (Fig. 2). Hence, appearance of spinel phase admixtures in samples calcined at high temperatures can be explained either by a partial decomposition of metastable alumina-containing perovskite-like solid solution or by interaction of amorphous alumina admixtures with the surface of perovskite particles. In the latter case, such an interaction can be facilitated

by the surface segregation of transition metal cations in low-temperature perovskite phases, up to generation of simple oxides admixtures as revealed by XRD in supported systems calcined at 900 °C (Table 1).

In any case, interaction of supported perovskites phases with corundum-support observed here is not so strong as observed in the case of γ-Al_2O_3-supported $LaMnO_3$ [5], when after annealing at 1100 °C $LaAlO_3$ and MnO_x phases were revealed.

X-ray microanalysis revealed that in the case of samples prepared via Pechini method, the active component forms a separate layer with thickness ∼60–160 μm covering the walls of monolithic support. The SEM data (Fig. 2) agree well with this estimation of the perovskite layer thickness being composed of large (10–100 μm) macroporous platelets separated by cracks. When the traditional wet impregnation method was used, the active component was distributed uniformly across the wall thickness (not shown for brevity).

According to TEM data, perovskite platelets are comprised of round or hexagonal particles with typical sizes in the range of 10–100 nm (Fig. 3). These crystals are certainly formed by stacking of microblocks as follows from smaller X-ray particle sizes (vide supra).

For all supported catalysts, the specific surface area was about 4–6 m^2/g independent upon the calcination temperature. While in the range of pore sizes exceeding 30 nm the pore size distribution was similar for both support and supported systems, the volume of narrow (<10 nm) pores was decreased for 0.05 cm^3/g due to perovskites supporting.

3.2. Catalytic activity

3.2.1. Methane combustion

Following the approach previously verified for bulk monolithic perovskites [9,10], the efficient first-order rate constants of methane combustion (k, s^{-1}) were estimated from the conversion values (x) by using the equation for the integral plug-flow reactor:

$$k = -\frac{\ln(1-x)}{\tau}$$

where τ is a relative contact time ($V_{cat.}/V_{flow}$) being equal to 0.25 s in the majority of experiments. The apparent activation energies calculated from the temperature dependence of those rate constants were found to vary within 20–25 kcal/mol range for all catalysts calcined at 700–900 °C. For supported lanthanum manganites, ferrites and nickelates, the apparent activation energy was the same even after annealing at 1100 °C, whereas it increases to ∼35 kcal/mol for lanthanum cobaltites and cuprates. Similar values of the activation energy ∼20 kcal/mol were obtained in this work for samples prepared via monolithic corundum-support wet impregnation with mixed nitrate/nitrate + citric acid solutions as well as by McCarty and Wise [11] for bulk perovskites powders. Hence, in conditions used in this work, methane deep oxidation proceeds in kinetically controlled region without any impact of the pore diffusion. It allows to analyze the effect of the samples chemical composition and structure on their performance.

Among supported catalysts, the highest level of activity was demonstrated by manganites and ferrites of lanthanum (Fig. 4a–c). After annealing at enhanced temperatures, activity declines, most strongly for lanthanum cobaltites, nickelates and cuprates. Since for the latter systems spinel phases emerge after annealing, this effect can be assigned to the surface blocking by those less reactive phases generated by any of the mechanism discussed above. In the case of lanthanum manganites and ferrites, activity decline with temperature is less pronounced which correlates with a lower amount of dissolved alumina and the absence of spinel admixtures in high-temperature phases. Activity decline for those phases certainly correlates with the decrease of the amount of reactive oxygen forms as revealed by TPR (vide infra).

Typical TPR results for lanthanum manganite containing systems are presented in Fig. 5. Several peaks of reduction observed here correspond to the surface (small peaks at $T \leq 230$ °C) and bulk (at ∼300–400 and ∼700–900 °C) reduction of a sample. Indeed, even for bulk $LaMnO_3$ sample (curve 1), the amount of oxygen removed up to 230 °C is less than 25% of monolayer. In general, these reactive surface oxygen forms can be located either at some surface defects or correspond to oxygen adsorption on the regular centers presented at some perovskite faces. In the middle and high-temperature peaks, ∼4.6 and ∼6 monolayers are removed from that sample, respectively, thus indicating its bulk reduction. For supported samples, the relative amount of oxygen removed in the low-temperature region is

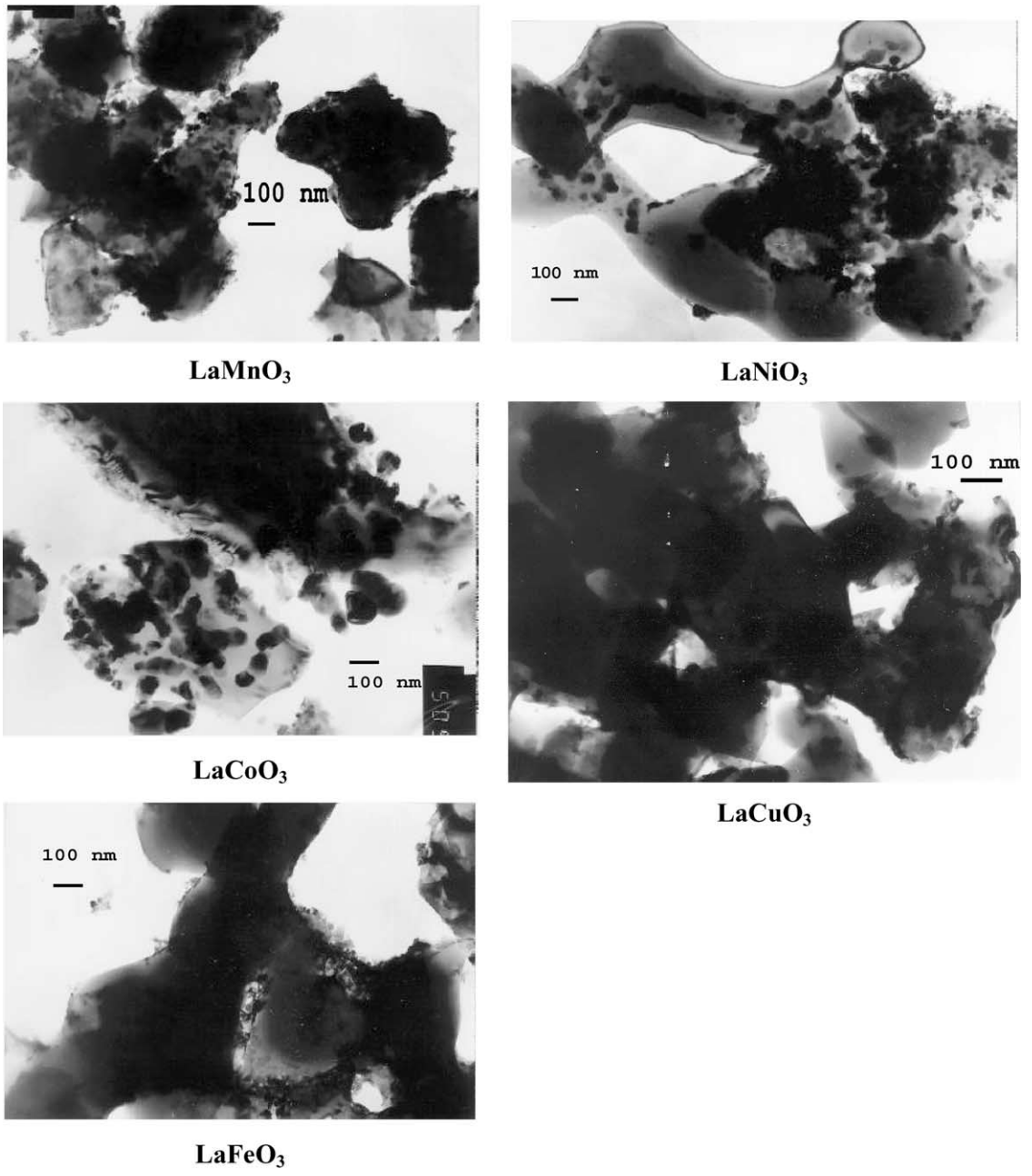

Fig. 3. TEM data on supported perovskites calcined at 700 °C.

compared with that for the bulk sample, decreasing with increasing of annealing temperature. According to the reduction balance, after 800–900 °C, all bulk manganese cations are reduced to Mn^{2+} state, which agrees with the green color of discharged samples. Earlier, TPR peaks in the low-temperature region were observed for MnO_x-supported catalysts [12], as well as for bulk $LaMnO_{3+\delta}$ [13] and $LaFeO_3$ [14]

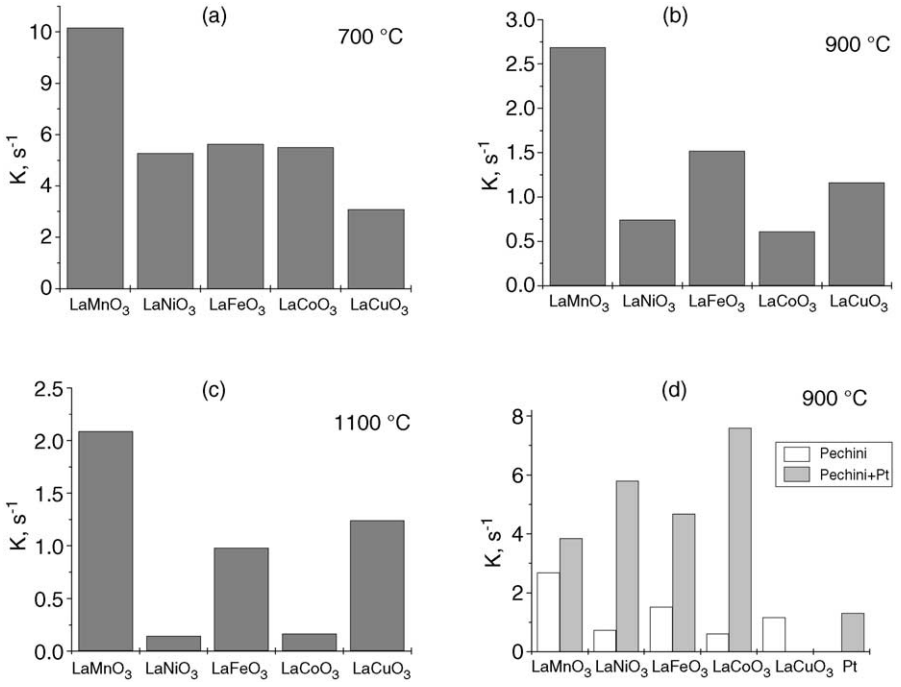

Fig. 4. Methane oxidation data at 625 °C (k, s^{-1}) versus perovskite chemical composition and calcination temperature.

perovskites calcined at moderate temperatures. Disappearance of the low-temperature (≤230 °C) peaks with the increase of the calcination temperature suggests either annealing of surface defects including segregated MnO_x clusters at the intergrain boundaries (mean XRD particle sizes increase with the temperature of annealing), or surface planes rearrangement into more densely packed less reactive structures. This suggestion is supported by the absence of any low-temperature TPR peaks for a sample of bulk lanthanum manganite perovskite studied in [15]. The annealing temperature affects even the middle- and high-temperature TPR peaks corresponding to bulk reduction of sample, implying the rearrangement of the bulk structure which requires further studies.

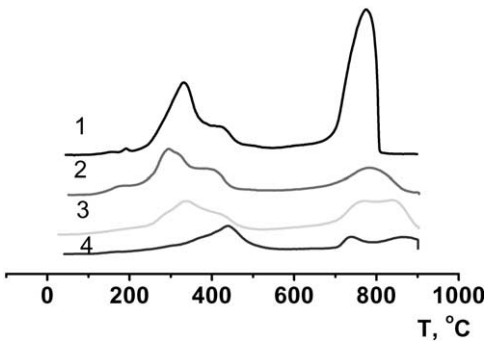

Fig. 5. TPR in H_2: 1, $LaMnO_3$ (bulk) at 800 °C; 2, $LaMnO_3/\alpha$-Al_2O_3 at 700 °C; 3, $LaMnO_3/\alpha$-Al_2O_3 at 900 °C; 4, $LaMnO_3/\alpha$-Al_2O_3 at 1100 °C.

Since in the range of temperatures up to 600 °C methane oxidation is controlled by the surface reaction (kinetics condition) and the mode of the active component distribution across the monolith wall is of no importance, activity of perovskites supported by the traditional impregnation method and those prepared via Pechini route differ only slightly (Fig. 6a and b). However, at enhanced temperatures, when the diffusion limitations in support pores is to be significant, samples prepared by Pechini method ensuring the surface location of the active component will demonstrate a higher performance.

Lanthanum manganite supported on corundum monolith was found to be more active as compared with Pt on the same support, though being less active

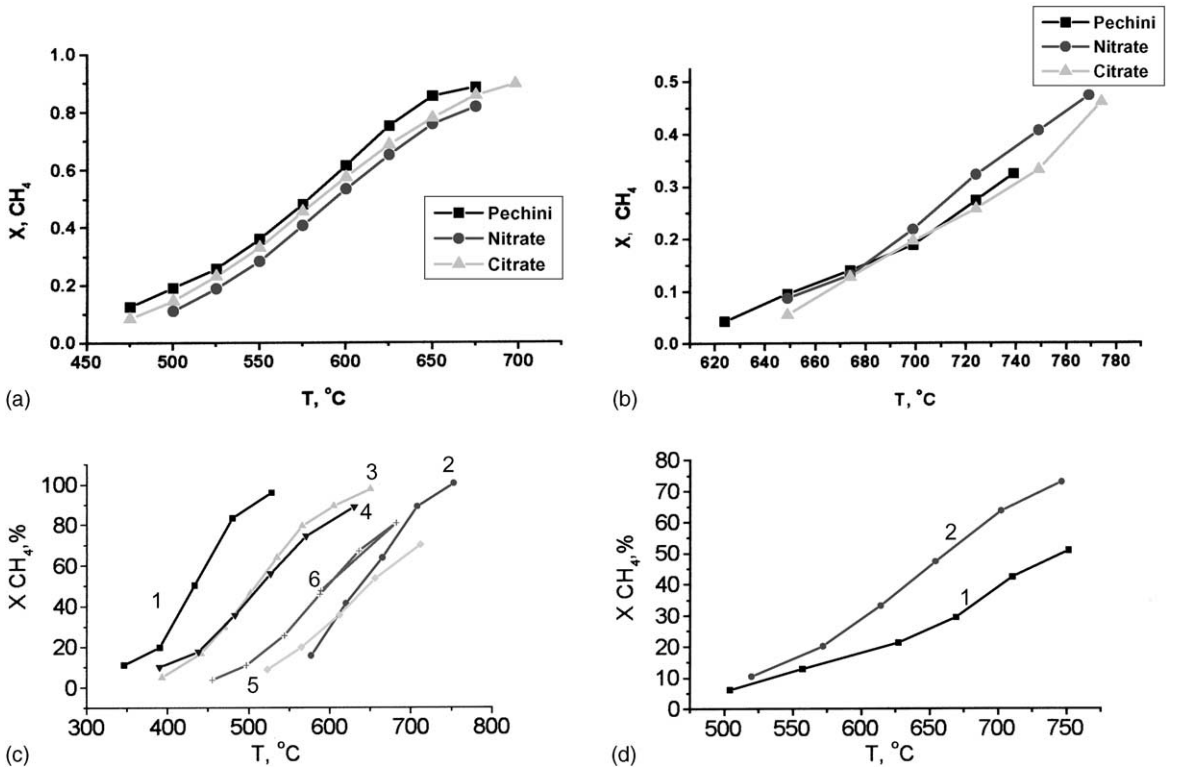

Fig. 6. Data on methane conversion for: (a) $LaCoO_3/\alpha$-Al_2O_3 catalysts prepared by different routes after calcination at 700 °C; (b) $LaCoO_3/\alpha$-Al_2O_3 catalysts prepared by different routes after calcination at 1100 °C; (c) 1, Pd/corundum at 700 °C; 2, Pt/corundum at 900 °C; 3, $LaMnO_3$/corundum at 700 °C; 4, $LaMnO_3$ + Pd/corundum at 700 °C; 5, $LaMnO_3$/corundum at 1100 °C; 6, $LaMnO_3$ + Pt/corundum at 1100 °C; (d) 1, $LaMnO_3$/corundum catalyst; 2, $LaMnO_3$ monolith [16] catalysts calcined at 900 °C, $\tau = 0.05$ s, wall thickness of honeycomb monolith was 0.3 mm.

in comparison with supported Pd (Fig. 6c). Supported perovskites modification by Pt was accompanied by the non-additive increase of activity, while Pd has no effect (Figs. 4d and 6c). The last feature can be tentatively assigned to deep oxidation of Pd after supporting on perovskites leading to its incorporation into the lattice.

At the same monolith shape and testing conditions, earlier developed and tested bulk monolithic perovskite samples [16] in the middle-temperature range usually possess somewhat higher activity as compared with supported systems (Fig. 6d). Thus, at 600 °C and standard reaction mixture composition (vide supra), for lanthanum manganite samples calcined at 900 °C, the reaction rate is equal to 2.76 and 4.5 mmol/g h for supported and bulk catalysts, respectively.

After high-temperature (1100 °C) annealing, the level of activity of corundum monolith-supported lanthanum manganite sample (17 wt.% $LaMnO_3$) exceeds that of 30 wt.% $LaMnO_3/\gamma$-Al_2O_3 sample [5]: at 600 °C, the rate of methane oxidation extrapolated to the standard feed composition is equal to 1.15 and 0.56 mmol/g h, resp. However, at a lower (800 °C) annealing temperature, the activity of γ-Al_2O_3-supported catalyst (11.8 mmol/g h at 600 °C) is certainly higher due to more developed surface area.

3.2.2. Partial oxidation of methane into syngas

In this reaction the most active and selective are cobalt and nickel-containing systems (Fig. 7), which agrees with the results of Shi et al. [17] and Pavlova et al. [18,19]. Those systems are certainly irreversibly

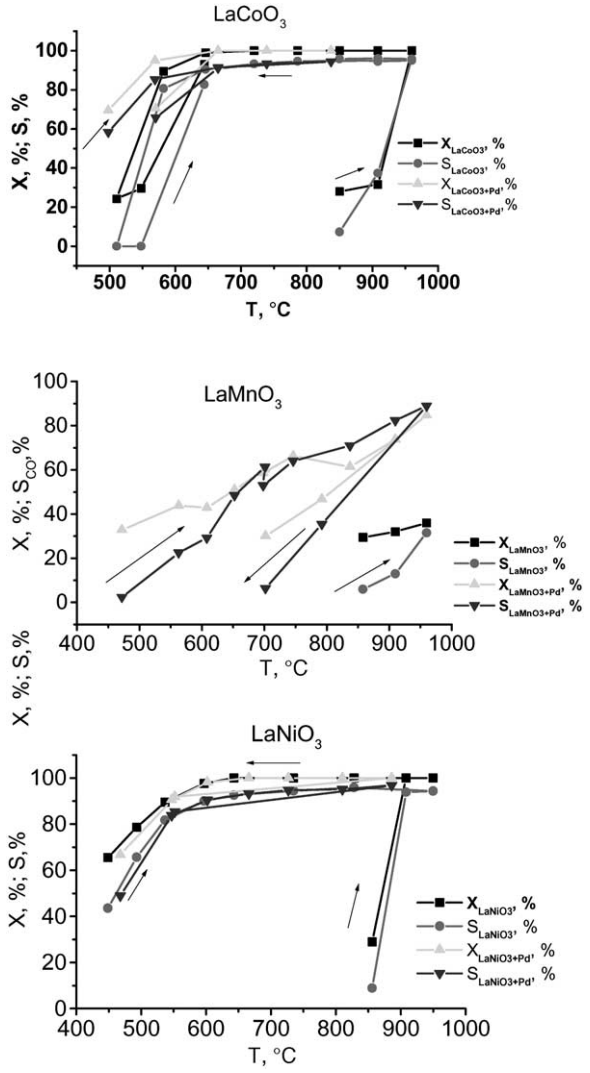

Fig. 7. Methane conversion and CO selectivity of supported perovskite and modified with Pd catalysts calcined at 700 °C in POM.

activated at high temperatures due to their reduction leading to surface segregation of small Co/Ni metallic clusters able to selectively convert methane into syngas [17–19]. This activation does not take place in the case of lanthanum manganite where such clusters could not be formed. Samples modification by Pd (∼0.2 wt.%) has a strong activation effect for all samples even including lanthanum manganite, which can be clearly explained by the methane activation on supported Pd clusters. Whereas for lanthanum cobaltite and nickelate the performance of activated samples only slightly depends upon the presence of Pd, for lanthanum manganites this effect is much stronger, though some deactivation is observed after keeping in the reaction media at high temperatures.

4. Conclusions

Pechini method was shown to be promising for preparation of corundum monolith-supported perovskites characterized by high thermal stability and enhanced performance in the high-temperature range where the pore diffusion limitations are of importance.

In the reaction of methane combustion, the most promising are supported lanthanum manganites and ferrites, which is explained by a less pronounced incorporation of aluminum cations into the lattice of those systems. In the reaction of methane selective oxidation into syngas, the highest activity and selectivity were obtained for lanthanum cobaltites and nickelates due to their ability to be easily reduced by methane forming surface metal clusters. Samples promotion by precious metals helps to increase their performance in both reactions.

Acknowledgements

The authors are thankful to Dr. G.N. Kryukova for performing TEM study.

References

[1] J.M.D. Tascon, L.J. Tejuca, React. Kinet. Catal. Lett. 15 (1980) 185.
[2] N. Yamazoe, Y. Teraoka, Catal. Today 8 (1990) 175.
[3] H. Arai, T. Yamada, K. Eguchi, Appl. Catal. 26 (1985) 265.
[4] S.N. Pavlova, N.F. Saputina, V.A. Sadykov, R.V. Bunina, V.P. Isupov, Patent of Russia No. 2,144,844 (2000).
[5] S. Cimino, L. Lisi, R. Pirone, G. Russo, M. Turco, Catal. Today 59 (2000) 19.
[6] M.P. Pechini, US Patent No. 3,330,697 (1967).
[7] V.V. Malakhov, A.A. Vlasov, Kinet. Catal. 36 (1995) 503 (in Russian).
[8] M. Kakihana, M. Yoshimura, Chem. Soc. Jpn. 72 (1999) 1427.
[9] D. Klvana, J. Vaillacourt, J. Kirchnerova, J. Chaouki, Appl. Catal. A 109 (1994) 181.

[10] P. Ciambelli, V. Palma, S.F. Tikhov, V.A. Sadykov, L.A. Isupova, L. Lisi, Catal. Today 47 (1999) 1999.
[11] J.G. McCarty, H. Wise, Catal. Today 8 (1990) 231.
[12] N.M. Popova, G.D. Kosmambetova, L.A. Sokolova, Z.T. Zeksembaeva, K.D. Dosumov, J. Phys. Chem. 75 (2001) 44.
[13] P. Ciambelli, S. Cimino, S. Rossi, M. Faticanti, L. Lisi, G. Minelli, I. Pettiti, P. Porta, G. Russo, M. Turco, Appl. Catal. B 24 (2000) 243.
[14] Z. Zhong, K. Chen, Y. Ji, Q. Yan, Appl. Catal. 156 (1997) 29.
[15] J.L.G. Fierro, J.M.D. Tascon, L. Gonzalez Tejuca, J. Catal. 89 (1984) 209.
[16] L.A. Isupova, G.M. Alikina, O.I. Snegurenko, V.A. Sadykov, S.V. Tsybulya, Appl. Catal. B 21 (1999) 171.
[17] K. Shi, H. Li, Y. Shang, G. Xu, Y. Wei, React. Kinet. Catal. Lett. 71 (2000) 177.
[18] S.N. Pavlova, V.A. Sadykov, N.F. Saputina, V.I. Zaikovskii, A.V. Kalinkin, G.N. Kustova, S.V. Tsybulya, V.A. Rogov, I.A. Zolotarslii, R.V. Bunina, in: Book of Abstracts of EuropoCat-IV, Rimini, Italy, 1999, p. 567.
[19] S.N. Pavlova, V.A. Sadykov, E.A. Paukshtis, E.B. Burgina, S.P. Degtyarev, D.I. Kochubei, A.V. Kalinkin, N.F. Saputina, R.I. Maximovskaya, V.I. Zaikovskii, R. Roy, D. Agrawal, Stud. Surf. Sci. Catal. 119 (1998) 759.